Puncture performance tests reveal distinct feeding modes in pinniped teeth

Carlos Mauricio Peredo[1,2,3,*], Danielle N. Ingle[2], and Christopher D. Marshall[2,3,4]

[1]Department of Earth and Environmental Science, University of Michigan, Ann Arbor, MI, USA

[2]Department of Marine Biology, Texas A&M University, Galveston Campus, Galveston, TX, USA

[3]Department of Paleobiology, National Museum of Natural History, Washington D.C., USA

[4]Department of Ecology and Conservation Biology, Texas A&M University, College Station, TX, USA

[*]Author for correspondence: cmperedo@umich.edu

Abstract

Marine mammals underwent a dramatic series of morphological transformations throughout their evolutionary history that facilitated their ecological transition to life in the water. Pinnipeds are a diverse clade of marine mammals that evolved from terrestrial carnivorans in the Oligocene (~27 Ma). However, pinnipeds have secondarily lost the dental innovations emblematic of mammalian and carnivoran feeding, such as a talonid basin or shearing carnassials. Modern pinnipeds do not masticate their prey, but can reduce prey size through chopping behavior. Typically, small prey are swallowed whole. Nevertheless, pinnipeds display a wide breadth of morphology of the post-canine teeth. We investigated the relationship between dental morphologies and pinniped feeding by measuring the puncture performance of the cheek-teeth of seven extant pinniped genera.

Puncture performance was measured as the maximum force and the maximum energy required to puncture a standardized prey item (*Loligo sp*). We report signficant differences in the puncture performance values across the seven genera, and identify three distinct categories based on cheek-teeth morphology and puncture performance: effective, ineffective, and moderate puncturers. In addition, we measured the overall complexity of the tooth row using two different metrics, Orientation Patch Count Rotated (OPCR) and Relif Index (RFI). Neither metric of complexity predicted puncture performance. Finally, we discuss these results in the broader context of known pinniped feeding strategies and lay the groundwork for subsequent efforts to explore the ecological variation of specific dental morphologies.

Introduction

Marine mammals are secondarily aquatic vertebrates that are ideal for studying drivers of morphological transformations and ecological transitions across a group's evolutionary history (Pyenson, 2017; Uhen, 2007). Pinnipeds are a monophyletic clade of marine carnivorans that evolved from terrestrial ancestors approximately 27 million years ago (Berta et al., 2018). Their evolutionary history is documented by a series of stem pinniped fossils that capture many changes in morphology that are associated with a marine environment (Berta et al., 2018).

The rise and success of mammals is often linked to the origin of two dentition-related key innovations: a differentiated dentition and a tribosphenic molar. These innovations facilitate precise occlusion of the upper and lower dentition, which co-evolves with the rise of mastication, which is a hallmark of mammalian feeding (Gregory, 1921; Herring, 1993; Herring et al., 2001; Hiiemae, 2000; Ungar, 2010; Weijs, 1994). Mastication is a highly specialized behavior with a precise definition that requires a power stroke of the lower jaw as well as precise occlusion

between the upper and lower dentition (Ahlgren, 1966; Herring, 1993; Herring et al., 2001; Hiiemae, 1978; Hiiemae, 2000; Weijs, 1994). Despite having descended from terrestrial mammals, extant pinnipeds lack a tribosphenic molar and do not masticate (Jones et al., 2013; Marshall and Goldbogen, 2016; Marshall and Pyenson, 2019). Although some pinnipeds do process prey by chopping, ripping, or tearing with their teeth (Hocking et al., 2017a), they lack the precise occlusion and the talonid basin emblematic of mastication. Instead, many extant pinnipeds have a dentition that is secondarily reduced or simplified, resulting in pinnipeds being described as homodont or functionally homodont by numerous authors (Berta et al., 2018; Jones et al., 2013; Marshall and Pyenson, 2019; Uhen, 2018). These changes are associated with a return to the aquatic environment and an emphasis on the use of teeth for prey capture over prey processing (Marshall and Pyenson, 2019). These changes and the resulting performance of cheek teeth for feeding by pinnipeds are of interest from an evolutionary and biomechanics perspective.

Although the dentition of extant pinnipeds has become simplified, lacks the precise occlusion characteristic of terrestrial mammals, and they do not masticate, there nevertheless remains a notable degree of variability in the morphology of pinniped cheek-teeth (Figure 1). The breadth of cheek-teeth morphology in pinnipeds ranges from simple conical pegs to complex, multi-cusped, trident shaped teeth, which include varying degrees of wear. These morphologies potentially relate to the diversity of pinniped feeding modes, which include raptorial biters, suction specialists, filter feeders, and multimodal generalists. These feeding modes can span multiple prey types including fish, squid, krill, and tetrapods (Marshall et al., 2008; Marshall and Pyenson, 2019; Marshall et al., 2014; Pauly et al., 1998). In terrestrial mammals, dental morphology is often used as a proxy for studying feeding ecology, especially for fossil specimens (e.g., Damuth and Janis, 2011; Gill et al., 2014; Luo et al., 2011).

To understand the relationship of varying dental morphologies with feeding in pinnipeds we conducted puncture performance tests, using models of the cheek-teeth of seven extant pinniped genera, as measured by the maximum force to puncture (F_{max}) and the maximum energy to puncture (E_{max}). We tested the hypothesis that different pinniped dental morphologies exhibit significant differences in their ability to puncture prey. We predicted that pinnipeds that use their teeth to capture prey raptorially would require the least force and energy to puncture, indicating that they are effective puncturers. Conversely, we predicted that pinnipeds that capture prey via suction would require the most force and energy to puncture and speculate that they may even be incapable of puncturing the prey item (ineffective puncturers). Finally, we predicted that more complex, multicusped teeth puncture prey intermediate to the simple, conical teeth of raptorial biters and that of suction feeders (i.e., moderate puncturers). In addition, we quantified the shape of cheek-teeth within each tooth row using Orientation Patch Count Rotated (OPCR) and Relief Index (RFI) and tested the hypothesis that these metrics correlate with puncture performance. We predicted that increased tooth complexity would be correlated with increased puncture performance (i.e. lower F_{max} and E_{max}).

Materials and Methods

Taxonomic Selection

To build a sample dataset with a phylogenetic context, we chose seven extant pinniped taxa (Families Phocidae and Otariidae) that spanned the breath of dental morphologies and known feeding ecologies. Our sample includes one specimen of each taxon, including four phocids (*Lobodon carcinophagus*, *Hydrurga leptonyx*, *Ommatophoca rossii*, *Mirounga leonina*) and three otariids (*Zalophus californianus*, *Callorhinus ursinus*, and *Arctocephalus pusillus*). This

taxonomic sampling includes specialized and generalized raptorial biters (*Zalophus californianus, Hydrurga leptonyx, Callorhinus ursinus,* and *Arctocephalus pusillus*) (Marshall et al., 2015b), specialized suction feeders (*Mirounga leonina, Ommatophoca rossii*) (Bryden and Felts, 1974; Hocking et al., 2013; Kienle and Berta, 2019; King, 1964), and filter feeders (*Lobodon carcinophagus*) (Hocking et al., 2013; Klages and Cockcroft, 1989; Marshall and Pyenson, 2019; Ross et al., 1976). We chose only adult specimens with a complete dentition that lacked any obvious pathologies or obvious abnormal phenotype. Each of the genera selected represent a minimal number of extant species, with similar feeding modes, with the exception of *Arctocephalus*. *Arctocephalus* is a diverse genus that includes as many as eight species (Brunner, 2004) and encompasses a wide diversity of feeding modes (Hoskins et al., 2015). Our results are therefore only informative for *Arctocephalus pusillus*, the only *Arctocephalus* species included in this study.

CT Scanning and 3D Printing

We scanned the skulls and mandibles in occlusion of each specimen using Nikon Metrology's combined 225/450 kV microfocus X-ray computed tomography (CT) walk-in vault system at National Technical Systems in Belcamp, Maryland, USA. Computed tomography slice thickness was 0.03mm. DICOM files were processed in Mimics (Materialise NV, Leuven, Belgium) and three-dimensional models of the cranium and mandibles were created. The 3D models of these skulls are archived on Zenodo at DOI: 10.5281/zenodo.5236563. The skull of *Arctocephalus pusillus* (NMV C5717) was scanned by the Evans EvoMorph lab using a Siemens Somatom GoUp medical CT scanner at Monash Biomedical Imaging, a technology research platform at Monash University, AU and is archived on Sketchfab: https://sketchfab.com/3d-models/skull-of-

the-australian-fur-seal-24b0f9ae93d94fb79fb203cd6b4ec5f9. The skull of *Zalophus californianus* was scanned at the University of Texas High-Resolution X-Ray Computed Tomography Facility using a Varian Medical Systems ACTIS scanner. Access to these data was provided by Blaire Van Valkenburgh and Tim Rowe via MorphoSource (Duke University) under NSF IOB-0517748 and DBI-1902242.

Each 3D model was manually trimmed to include only the dental arcade of the post-canine cheek-teeth and then 3D printed at full scale by Shapeways (New York, New York, USA) using the "Versatile Plastic" option and a natural finish. We manually inspected each print for quality and signs of anomalies during the printing process. We chose "Versatile Plastic" to ensure a consistent and standard material across each print, not to mimic the material properties of enamel. This ensured that our methodology is easy to replicate for both extant and fossil specimens for future work.

Puncture Performance Testing

3D printed tooth rows were attached to 25.0 mm diameter steel, rectangular tubing cut into sections ranging from 57.2–123.3 mm in length. Tooth rows were attached to these steel sections using Sonic-Weld epoxy putty (Tallahassee, FL, USA) and cured at room temperature (20–22^{o}C) for 24 hrs. The 3D print-epoxy was reinforced with industrial-strength cyanoacrylate. The distance from the base of the steel tubing and the longest cusp apex ranged from 50.8–71.1 mm, and tooth cusps were set orthogonally to the steel section base.

Restaurant grade market squid (*Loligo sp.*) was chosen since squid are a prey item that is consistently consumed by most pinnipeds (Pauly et al., 1998). Also, squid mantles represent a relatively homogenous biological structure that allowed us to control for variation in tissue

properties compared to the more hetergeneous structures of fishes. For example, Whitenack and Motta (2010) showed that varying fish scale thickness significantly changed tooth puncture performance of shark teeth. Squid were received and stored frozen, then thawed at room temperature for 4–6 hours prior to puncture performance testing. We measured squid mantle lengths in ImageJ (Abràmoff et al., 2004) as the distance from the tip of the mantle collar to the posterior end of the mantle; these values ranged from 111.22 mm–201.5 mm. Prior to testing, squid were placed on a wooden table lined with sandpaper (120 grit) to prevent movement during puncture tests following Whitenack and Motta (2010). To prevent inconsistent puncture through shifting of the internal pen, squid mantles were oriented 30^{o} clockwise to their longitudinal axis and positioned so that the apex of the centermost tooth (rows with five teeth) or the location between the two centermost-teeth (rows with four teeth) was aligned with the center, or longitudinal axis of the squid mantle (Figure 2). Each trial began with the longest apex of every tooth row positioned 50 mm above the squid mantle. A c-clamp was used to attach the steel tubing and tooth rows to the MTS grip and 2.5kN load cell of the MTS Insight 5 system (Eden Prairie, MN, USA; Figure 2). For each puncture trial, tooth rows were driven into the mantle of the squid at a displacement rate of 15.00 mm/s. The sampling rate of the MTS machine was 10 Hz.

For each tooth row, five squid were punctured for a total of 10 puncture performance trials per treatment (2 trials/squid). For the first trial for each individual squid, the pen was left intact and the tooth row driven in at the location where the center tooth (or the location between the two centermost teeth) aligned with 25% of the mantle length. In preparation for the second trial, the pen was manually removed from the mantle; no cutting was required. Here, the tooth row punctured the mantle at 75% of the mantle length, parallel to the first puncture site (Figure 2).

Load-displacement data was collected in TestWorks4 software (version 4.11 MTS, Eden Prairie, MN, USA). Maximum puncture force (F_{max}) and energy to maximum puncture force (E_{max}) were calculated using TestWorks4 software. Load-displacement curves from preliminary tests showed no drop in load at the end of the test when teeth punctured the squid mantle. Therefore, tooth row displacements, or the vertical distance moved, was terminated when the longest tooth apex of each row reached a distance of 3 mm above the wooden specimen support table (Figure 2). This protocol ensured standardization of puncture distance and also prevented damage to the load cell or 3D printed models. Each 3D print was visually inspected for signs of deformation or degradation after each trial and no such concerns were observed.

Measures of Dental Morphology

To further understand the extent to which morphology explained our performance results, we quantified the shape of the tooth crowns using two established morphometric measurements: Orientation Patch Count Rotated (OPCR) and Relief Index (RFI). OPCR is a geographic information system analysis developed by Evans et al. (2007) and refined by Evans and Janis (2014). This method measures the dental complexity of a tooth or tooth row by binning continuously adjacent faces of identical orientation into patches and then measuring number of distinct patches on the model. Using this metric, higher OPCR scores indicate more variation in the topography of the tooth or tooth row, with many distinct patches each with distinct orientations. Conversely, lower OPCR scores represent a simpler model overall, with large patches of homogeneous regions all facing the same orientation. The lowest possible OPCR score is 8, which represents a perfect cone with faces all binned into 8 arbitrary directions.

Unlike OPCR, which measures dental complexity, RFI measures the overall height of the crown. The original RFI formula, first used by Ungar and M'Kirera (2003), was a simple ratio of the tooth crown's surface area to the 2D footprint area. More recently, authors have altered this formula so that RFI instead applies transformations to these two values (Boyer, 2008; Pampush et al., 2016). In each case, the method is comparing the three-dimensional surface area of the tooth crown to the two-dimensional footprint at the crown's base. Using this metric, a ratio of 1 indicates a very tall tooth, with a high 3D surface area relative to its 2D footprint, while a ratio that approaches 0 indicates a shorter tooth, with a large 2D footprint relative to its 3D surface area. Here, we follow the best practices suggested by Pampush et al. (2016) and use the weighted ratio version of the metric (Boyer, 2008).

We measured OPCR and RFI using the R package molaR (Pampush et al., 2016), which was created specifically for quantitative topographic analyses of teeth. The 3D surface models of each tooth row were trimmed to include only the crowns. Then, the models were simplified to a standard number of faces (1,000) and oriented such that the occlusal surface was aligned with the Z axis. The molaR R package was used to measure OPCR and RFI following Pampush et al. (2016). Our R code is provided in the electronic supplemental materials (ESM).

Statistics

All data were tested for normality using a Shapiro-Wilk's test (Shapiro and Wilk, 1965) and subsequently log transformed. A Pearson correlation was conducted between squid mantle length and the maximum force to puncture (F_{max}) and maximum energy to puncture (E_{max}) to test whether mantle length significantly impacted puncture performance metrics. To determine significant differences ($\alpha \leq 0.05$) in the F_{max} and the E_{max} we considered each tooth row

separately, as they were used in the experimental trials. Therefore, because our study includes seven species, we considered 14 total tooth rows (seven upper tooth rows and seven lower tooth rows). A one-way MANOVA was performed to test the independent variable (tooth row) against the two dependent variables (F_{max} and E_{max}). A second one-way MANOVA was conducted to test the independent variable (Pen *in situ* vs. pen excised) against the two dependent variables (F_{max} and E_{max}). Both one-way MANOVAs used the entire dataset including all trials with the pen *in situ* and with the pen excised. A Pearson correlation plotted both metrics of dental complexity (OPCR and RFI) against the F_{max} and E_{max} to test for correlation between dental complexity and puncture performance metrics. All statistical tests were conducted using the R package DPLYR (Wickham et al., 2016).

Results

Squid Mantle Length

The smallest squid mantle in these experiments measured 111.2 mm, and the largest measured 201.5 mm. The mean mantle length was 146.2 mm (s.d. ± 22.3 mm). To test whether the squid's mantle length potentially biased results, we conducted a Pearson correlation of mantle length against the maximum force to puncture and the maximum energy to puncture for each trial. We found no correlation between squid mantle length and maximum force to puncture (Pearson's r = -0.117; t = -0.974; df = 68; p-value = 0.334). Similarly, we found no correlation between squid mantle length and maximum energy to puncture (Pearson's r = -0.080; t = -0.663; df = 68; p-value = 0.510). Thus, squid mantle length had no correlation with the puncture performance metrics measured.

Puncture Performance

We conducted a one-way MANOVA to test for significant differences ($\alpha \leq 0.05$) between the independent variable (tooth row) against the two dependent variables (F_{max} and E_{max}) using a Pillai's Trace test. The tooth row had a statistically significant association with both F_{max} and E_{max} (Pillai's Trace = 0.954; $F(26, 252)$; $p < 0.0001$). A subsequent one-way MANOVA was conducted to test for significant differences ($\alpha \leq 0.05$) between the independent variable (pen *in situ* vs pen excised) against the two dependent variables (F_{max} and E_{max}), also using a Pillai's Trace test. The presence of the pen had a statistically significant association with both F_{max} and E_{max} (Pillai's Trace = 0.113; $F(2, 137)$; $p = 2.59 \times 10^{-4}$). Therefore, both independent variables had a significant association with both the maximum force to puncture (Figure 3; Tables 1, 2) and maximum energy to puncture (Figure 4; Tables 3, 4). Two post-hoc Tukey's HSD tests were conducted to compare differences in the maximum force (Table S3) and maximum energy (Table S4) to puncture among the different tooth rows. These post-hoc tests demonstrate significant differences (Table S2) between the best performing tooth rows (e.g., *Hydrurga* lowers, *Zalophus* lowers) and the worst performing tooth rows (*Lobodon* lowers, *Ommatophoca* lowers).

Puncture performance data show key patterns that . broadly split the seven genera into three distinct performance groups. The most effective puncturers (lowest force and energy to penetrate) included *Callorhinus*, *Zalophus*, and *Hydrurga*; each of these taxa had at least one set of teeth which punctured with overall low force values (for example, a mean from the five performance trials of less than 20 N with the pen *in situ*). The next group, which included *Arctocephalus*, *Mirounga*, and *Lobodon*, are moderate puncturers. These taxa had some trials where the maximum force to puncture approached those of the first group, but altogether the mean and the standard error of the five trials was greater, suggesting that this second group is

capable of strong puncture performance, but were more variable and less consistent than the first group. Finally, *Ommatophoca* was an ineffective puncturer that required the greatest maximum force to puncture compared to the other genera in this study; the mean maximum force to puncture of its five performance trials > 40 N with the pen *in situ*.

The lower dentition of five of the seven genera (*Callorhinus*, *Zalophus*, *Arctocephalus*, *Mirounga*, and *Hydrurga*) in this experiment performed better than the upper dentition. This difference was particularly pronounced in *Callorhinus* and *Zalophus*; each of these taxa had no overlap among any of the trials for their upper and lower dentition. Conversley, *Ommatophoca* and *Lobodon* each performed better with the upper dentition, with *Lobodon* in particular exhibiting a greater discrepancy between the force and energy required to puncture for the upper and lower tooth rows.

Measures of Dental Morphology

Of the two metrics used to quantify the overall shape of the tooth row, OPCR values ranged from 47.0 (*Mirounga*) to 112.6 (*Hydrurga*) (Figures 1 and 5). The multicusped pinnipeds (*Hydrurga* and *Lobodon*) exhibited the greatest OPCR values, whereas the more conical shaped teeth had the lowest OPCR values (*Mirounga* and *Arctopcephalus*). We found no correlation between dental complexity (OPCR) and the maximum force to puncture (Pearson's r = -0.024; t = -0.083; df = 12; p-value = 0.936), nor between dental complexity (OPCR) and maximum energy to puncture (Pearson's r = 0.198; t = 0.702; df = 12; p-value = 0.496).

RFI values ranged from 0.144 (*Ommatophoca*) to 0.393 (*Lobodon*) (Figures 1 and 6). The lowest RFI values were *Ommatophoca and Mirounga.* Both taxa exhibited heavy wear of the dental crowns and lacked accessory cusps, which is typical of adult specimens of these species

(King, 1983; pers. obs., respectively). The multicusped teeth of *Hydrurga* and *Lobodon* resulted in similar RFI values to those of *Arctocephalus* and *Zalophus*, suggesting that multiple cusps alone do not necessarily increase RFI values. The teeth of *Callorhinus* yielded intermediate RFI values, suggesting that although the crown is quite tall, a relatively broad base lowers the RFI value. We found no correlation between crown height (RFI) and the maximum force to puncture (Pearson's r = -0.429; t = -1.644; df = 12; p-value = 0.126), nor between crown height (RFI) and the maximum energy to puncture (Pearson's r = -0.248; t = -0.887; df = 12; p-value = 0.393)..

Discussion

Extant pinnipeds do not masticate and they lack a dentition specialized for precise occlusion (Marshall and Pyenson, 2019), such as that seen in ungulates, primates, and rodents (Boyer, 2008; Evans and Janis, 2014; Evans et al., 2007; Ungar, 2010; Winchester et al., 2014). Despite this, pinnipeds, particularly phocids, display a high degree of variability in their cheek-teeth morphology (Figure 1). Previous studies have sought to describe trends in the evolution of pinniped feeding by correlating dental morphotypes with specific feeding ecologies (Adam and Berta, 2002; Boessenecker, 2011; Churchill and Clementz, 2015a; Churchill and Clementz, 2015b; Hocking et al., 2017b; Hocking et al., 2017c; Kienle and Berta, 2016; Kienle and Berta, 2019; Kienle et al., 2017; King, 1961; King, 1969; King, 1983; Ross et al., 1976). However, to date there is a notable lack of experimental work that test functional hypotheses. Here, we test whether specific dental morphologies are better at prey puncture. Our results demonstrate significant differences in puncture performance (both F_{max} and E_{max}) among the seven genera in this study. Specifically, we identify three distinct functional groups based on their cheek-teeth

morphology and puncture performance: effective puncturers, ineffective puncturers, and moderate puncturers.

Callorhinus, *Zalophus*, and *Hydrurga*, are all effective puncturers. This group had the best performing set of cheek-teeth (defined as the minimal force or energy to puncture the prey item); they consistently required <20N of force to puncture and sometimes <10N. This group also encompasses the most disparate dental morphologies, from the conical teeth of *Callorhinus* to the multicusped teeth of *Hydrurga*. Based on known feeding performance, *Callorhinus* is a specialist raptorial biter that does not employ suction to capture food (Marshall et al., 2015a). Conversley, *Hydrurga* feeds on many different types of prey that range from penguins to krill, and is capable of multimodal feeding that includes raptorial biting (including grip and tear), suction, and filter feeding (Hocking et al., 2013; Kienle and Berta, 2016; Krause et al., 2015). Our results demonstrate that the dental morphologies of these taxa require less force and less energy to puncture prey.

The group of ineffective puncturers includes *Ommatophoca* and *Mirounga*. Both taxa required greater force to puncture the squid (>20N) and exhibited more variation in performance, sometimes requiring forces in excess of 40N. Although only a few feeding performance tests have been conducted (Naito et al., 2013), *Ommatophoca* and *Mirounga* are known suction feeders and their teeth are known to exhibit heavy wear from an early ontogenetic age (Bryden and Felts, 1974; Churchill and Clementz, 2015b; Kienle and Berta, 2016; King, 1964; Marshall and Pyenson, 2019; McGovern et al., 2019; Nordøy and Blix, 2000; van den Hoff and Thalmann, 2020). However, they typically swallow their prey whole, and the dental wear is the result of abrasion from suction, similar to that seen in walruses (Kastelein et al., 1994; Marshall and Pyenson, 2019). Thus, there is a potentially minimal loading environment on their cheek-teeth.

Our results suggest that there may be little to no selective pressure for piercing on the morphology and function of their cheek-teeth.

The third group, *Arctocephalus* and *Lobodon*, are moderate puncturers. *Arctocephalus* did not perform as well as *Callorhinus* and *Zalophus*, despite teeth that superficially resemble those of the more effective puncturers (tall, triangular shaped teeth). As with the suction feeders in this study, *Arctocephalus* puncture performance was more variable than those of the raptorial biters. *Arctocephalus* is a diverse genus that includes as many as eight species (Brunner, 2004). The taxon in our study, *Arctocephalus pusillus*, is sometimes characterized as a benthic forager based on diving records (Arnould and Costa, 2006; Arnould and Hindell, 2001; Deagle et al., 2009), but is known to target a wide range of both benthic and pelagic prey types (Deagle et al., 2009; Gales and Pemberton, 1994; Hoskins et al., 2015; Hume et al., 2004; Kirkwood et al., 2008; Littnan et al., 2007), suggesting that it is best characterized as a generalist feeder. Some evidence suggests that prey type, rather than where in the water column the prey is obtained, is a greater factor is how the prey is processed (Hocking et al., 2016). Our results suggest that the teeth of *Callorhinus* and *Zalophus* are better puncture performers relative to the more generalist teeth of *Arctocephalus pusillus*. These results substantiate performance data that claim *Callorhinus* is a biting specialist (Marshall et al., 2015b). The performance values for *Lobodon* were the most variable of the taxa in our study: maximum force to puncture ranged from 21N to >80N. *Lobodon* is known to ingest and subsequently filter krill, likely using suction and hydraulic jetting feeding modes (Klages and Cockcroft, 1989; Marshall and Pyenson, 2019; Ross et al., 1976). Our results suggest that, although the teeth of *Lobodon* do sometimes perform well in puncture experiments, their teeth exhibit a high variability in their capacity to puncture.

Although our results indicate distinct patterns based on their capacity to puncture, none of the tooth rows in our study failed to pierce the squid. We chose squid because they are a prey item consistently consumed by pinnipeds (Pauly et al., 1998) and because we expected it to be a soft, homogenous prey item. However, our results showed significant differences in the maximum force and maximum energy to puncture between trials with and without the pen, indicating that the squid pen is harder than we anticipated. Recent authors (Franco-Moreno et al., 2021) have reported resistance values for squid that are comparable to some teleost fishes, suggesting that it may not be as homogenous as previously thought. Now that a baseline of puncture performance using squid has been completed, follow up studies should use fish, especially considering that squid with the pen removed is not a biologically relevant sample prey item. Fish can have an overall greater tissue hardness relative to squid, and can provide a greater challenge to puncture performance (Franco-Moreno et al., 2021). Fish represent a more heterogeneous structure with a mix of hard and soft tissues. Such performance tests will likely discriminate feeding modes further, while establishing potential dietary constraints imposed by tooth morphology.

The presence of distinct cheek-teeth morphologies with distinct functional capabilities is interesting given that pinnipeds lack the talonid basin and precise occlusion characteristic of their terrestrial ancestors. Understanding our work in the broader context of the evolutionary biomechanics of mammalian feeding will require substantial comparative work. The physical constraints of feeding in an aquatic vs. terrestrial system poses many challenges. However, there are interesting questions regarding the changes in feeding performance in the transition to aquatic environments that can be elucidated. Our experiments demonstrate that these distinct morphologies differ in their capacity to puncture, but not all pinniped species necessarily use the cheek teeth during feeding. Further work might compare puncture performance metrics to

experimentally measured bite forces in pinnipeds, to test whether the forces required to puncture are within the range of what living pinnipeds can produce, and to link behavioral data with our experimental results.Finally, future work comparing the puncture performance and dental complexity of extant pinnipeds to that of stem pinniped ancestors and terrestrial carnivorans may elucidate the timing and mechanisms for the loss of mastication in pinnipeds.

Acknowledgments

We thank N.D. Pyenson and D.J. Bohaska for facilitating access to specimens at the NMNH. We also thank the Evans Morphology Lab, D.P. Hocking, and A.R. Evans for access to the *Arctocephalus* dataset and B. Van Valkenburgh and T. Rowe for access to the *Zalophus* dataset. Finally, we thank National Technical Systems (Belcamp, Maryland, USA) and C. Peitsch, R. Peitsch, and C. Schueler for providing access and resources for microCT scanning. We thank R. Perkins III (TAMUG) for help with specimen preparation for puncture tests.

Competing Interests

We declare no competing interests.

Author Contributions

All authors conceived and designed experiments, analyzed the data, contributed materials and tools, wrote the paper, and prepared figures. D.N.I. performed the experiments and collected the data. C.D.M. and C.M.P. CT scanned the specimens.

Funding

CMP was supported by the Remington Kellogg Fund and the Basis Foundation. CMP was further supported by National Science Foundation Award #1906181 and by the University of Michigan Society of Fellows. DNI was supported by a Texas A&M University, Galveston Campus Postdoctoral Scientist Fellowship. The funders had no role in the study design, data collection and analysis, decision to publish, or preparation of the manuscript.

Literature Cited

Abràmoff, M. D., Magalhães, P. J. and Ram, S. J. (2004). Image processing with ImageJ. *Biophotonics international* **11**, 36-42.

Adam, P. J. and Berta, A. (2002). Evolution of prey capture strategies and diet in the Pinnipedimorpha (Mammalia, Carnivora). *Oryctos* **4**, 83-107.

Ahlgren, J. (1966). Mechanism of mastication. *Acta Odontol. Scand.* **24**, 1–109.

Arnould, J. and Costa, D. (2006). Sea lions in drag, fur seals incognito: insights from the otariid deviants. In *Sea lions of the world: proceedings of the symposium sea lions of the world: conservation and research in the 21st Century*, pp. 309-323: Citeseer.

Arnould, J. P. and Hindell, M. A. (2001). Dive behaviour, foraging locations, and maternal-attendance patterns of Australian fur seals (*Arctocephalus pusillus doriferus*). *Canadian Journal of Zoology* **79**, 35-48.

Berta, A., Churchill, M. and Boessenecker, R. W. (2018). The Origin and Evolutionary Biology of Pinnipeds: Seals, Sea Lions, and Walruses. *Annual Review of Earth and Planetary Sciences* **46**, 203-228.

Boessenecker, R. W. (2011). New records of the fur seal *Callorhinus* (Carnivora: Otariidae) from the Plio-Pleistocene Rio Dell Formation of Northern California and comments on otariid dental evolution. *Journal of Vertebrate Paleontology* **31**, 454-467.

Boyer, D. M. (2008). Relief index of second mandibular molars is a correlate of diet among prosimian primates and other euarchontan mammals. *Journal of Human Evolution* **55**, 1118–1137.

Brunner, S. (2004). Fur seals and sea lions (Otariidae): identification of species and taxonomic review. *Systematics and Biodiversity* **1**, 339-439.

Bryden, M. and Felts, W. (1974). Quantitative anatomical observations on the skeletal and muscular systems of four species of Antarctic seals. *Journal of anatomy* **118**, 589.

Churchill, M. and Clementz, M. T. (2015a). The evolution of aquatic feeding in seals: insights from Enaliarctos (Carnivora: Pinnipedimorpha), the oldest known seal. *J Evol Biol*.

Churchill, M. and Clementz, M. T. (2015b). Functional implications of variation in tooth spacing and crown size in Pinnipedimorpha (Mammalia: Carnivora). *The Anatomical Record* **298**, 878-902.

Damuth, J. and Janis, C. M. (2011). On the relationship between hypsodonty and feeding ecology in ungulate mammals, and its utility in palaeoecology. *Biological Reviews* **86**, 733-758.

Deagle, B. E., Kirkwood, R. and Jarman, S. N. (2009). Analysis of Australian fur seal diet by pyrosequencing prey DNA in faeces. *Molecular ecology* **18**, 2022-2038.

Evans, A. R. and Janis, C. M. (2014). The eolution of high dental complexity in the horse lineage. *Annales Zoologici Fennici* **51**, 73-79.

Evans, A. R., Wilson, G. P., Fortelius, M. and Jernvall, J. (2007). High-level similarity of dentitions in carnivorans and rodents. *Nature* **445**, 78–81.

Franco-Moreno, R. A., Polly, P. D., Toro-Ibacache, V., Hernández-Carmona, G., Aguilar-Medrano, R., Marín-Enríquez, E. and Cruz-Escalona, V. H. (2021). Bite force in four pinniped species from the west coast of Baja California, Mexico, in relation to diet, feeding strategy, and niche differentiation. *Journal of Mammalian Evolution* **28**, 307-321.

Gales, R. and Pemberton, D. (1994). Diet of the Australian fur seal in Tasmania. *Marine and freshwater research* **45**, 653-664.

Gill, P. G., Purnell, M. A., Crumpton, N., Brown, K. R., Gostling, N. J., Stampanoni, M. and Rayfield, E. J. (2014). Dietary specializations and diversity in feeding ecology of the earliest stem mammals. *Nature* **512**, 303-305.

Gregory, W. K. (1921). The origin and evolution of the human dentition: a palaeontological review. *Journal of Dental Research* **3**, 87–228.

Herring, S. W. (1993). Functional morphology of mammalian mastication. *American Zoologist* **33**, 289–299.

Herring, S. W., Rafferty, K. L., Liu, Z. J. and Marshall, C. D. (2001). Jaw muscles and the skull in mammals: the biomechanics of mastication. *Comparative Biochemistry and Physiology Part A: Molecular & Integrative Physiology* **131**, 207–219.

Hiiemae, K. (1978). Mammalian mastication: a review of the activity of the jaw muscles and the movements they produce in chewing. *Development, function and evolution of teeth*, 359-398.

Hiiemae, K. M. (2000). Feeding in mammals. In *Feeding: Form, function, and evolution in tetrapod vertebrates*, vol. 1(ed. K. Schwenk), pp. 411–448. San Diego, CA: Academic Press.

Hocking, D. P., Evans, A. R. and Fitzgerald, E. M. G. (2013). Leopard seals (Hydrurga leptonyx) use suction and filter feeding when hunting small prey underwater. *Polar Biology* **36**, 211-222.

Hocking, D. P., Fitzgerald, E. M. G., Salverson, M. and Evans, A. R. (2016). Prey capture and processing behaviors vary with prey size and shape in Australian and subantarctic fur seals. *Marine Mammal Science* **32**, 568-587.

Hocking, D. P., Ladds, M. A., Slip, D. J., Fitzgerald, E. M. and Evans, A. R. (2017a). Chew, shake, and tear: prey processing in Australian sea lions (Neophoca cinerea). *Marine Mammal Science* **33**, 541-557.

Hocking, D. P., Marx, F. G., Park, T., Fitzgerald, E. M. G. and Evans, A. R. (2017b). A behavioural framework for the evolution of feeding in predatory aquatic mammals. *Proceedings of the Royal Society B: Biological Sciences* **284**.

Hocking, D. P., Marx, F. G., Park, T., Fitzgerald, E. M. G. and Evans, A. R. (2017c). Reply to comment by Kienle et al. 2017. *Proceedings of the Royal Society B: Biological Sciences* **284**, 20171836.

Hoskins, A. J., Costa, D. P. and Arnould, J. P. (2015). Utilisation of intensive foraging zones by female Australian fur seals. *PLoS ONE* **10**, e0117997.
Hume, F., Hindell, M., Pemberton, D. and Gales, R. (2004). Spatial and temporal variation in the diet of a high trophic level predator, the Australian fur seal (Arctocephalus pusillus doriferus). *Marine Biology* **144**, 407-415.
Jones, K. E., Ruff, C. B. and Goswami, A. (2013). Morphology and biomechanics of the pinniped jaw: mandibular evolution without mastication. *Anat Rec (Hoboken)* **296**, 1049-63.
Kastelein, R., Muller, M. and Terlouw, A. (1994). Oral suction of a Pacific walrus (*Odobenus rosmarus divergens*) in air and under water. *Zeitschrift fur Saugetierkunde* **59**, 105–115.
Kienle, S. S. and Berta, A. (2016). The better to eat you with: the comparative feeding morphology of phocid seals (Pinnipedia, Phocidae). *J Anat* **228**, 396-413.
Kienle, S. S. and Berta, A. (2019). The evolution of feeding strategies in phocid seals (Pinnipedia, Phocidae). *Journal of Vertebrate Paleontology*, e1559172.
Kienle, S. S., Law, C. J., Costa, D. P., Berta, A. and Mehta, R. S. (2017). Revisiting the behavioural framework of feeding in predatory aquatic mammals. *Proceedings of the Royal Society B: Biological Sciences* **284**, 20171035.
King, J. E. (1961). The feeding mechanism and jaws of the crabeater seal (*Lobodon carcinophagus*). *Mammalia* **25**, 462–466.
King, J. E. (1964). Swallowing modifications in the Ross seal. *Journal of anatomy* **99**, 206–207.
King, J. E. (1969). Some aspects of the anatomy of the Ross seal, Ommatophoca rossi (Pinnipedia: Phocidae).
King, J. E. (1983). Seals of the world. Ithaca, NY: Cornell University Press.
Kirkwood, R., Hume, F. and Hindell, M. (2008). Sea temperature variations mediate annual changes in the diet of Australian fur seals in Bass Strait. *Marine Ecology Progress Series* **369**, 297-309.
Klages, N. W. and Cockcroft, V. G. (1989). Feeding behaviour of a captive crabeater seal. *Polar biology (Print)* **10**, 403-404.
Krause, D. J., Goebel, M. E., Marshall, G. J. and Abernathy, K. (2015). Novel foraging strategies observed in a growing leopard seal (*Hydrurga leptonyx*) population at Livingston Island, Antarctic Peninsula. *Animal Biotelemetry* **3**, 1-14.
Littnan, C., Arnould, J. and Harcourt, R. (2007). Effect of proximity to the shelf edge on the diet of female Australian fur seals. *Marine Ecology Progress Series* **338**, 257-267.
Luo, Z.-X., Yuan, C.-X., Meng, Q.-J. and Ji, Q. (2011). A Jurassic eutherian mammal and divergence of marsupials and placentals. *Nature* **476**, 442-445.
Marshall, C. D. and Goldbogen, J. A. (2016). Marine Mammal Feeding mechanisms. In *Marine Mammal Physiology: Requisites for Ocean Living*, eds. M. A. Castellini and J.-A. Mellish), pp. 95–118. Boca Raton, FL: CRC Press.
Marshall, C. D., Kovacs, K. M. and Lydersen, C. (2008). Feeding kinematics, suction and hydraulic jetting capabilities in bearded seals (*Erignathus barbatus*). *Journal of Experimental Biology* **211**, 699–708.
Marshall, C. D. and Pyenson, N. D. (2019). Feeding in aquatic mammals: an evolutionary and functional approach. In *Feeding in Vertebrates*, eds. V. Bels and I. Q. Whishaw), pp. 743–785. Switzerland: Springer.

Marshall, C. D., Rosen, D. and Trites, A. W. (2015a). Feeding kinematics and performance of basal otariid pinnipeds, Steller sea lions (Eumetopias jubatus), and northern fur seals (Callorhinus ursinus): implications for the evolution of mammalian feeding. *Journal of Experimental Biology*.

Marshall, C. D., Rosen, D. A. and Trites, A. W. (2015b). Feeding kinematics and performance of basal otariid pinnipeds, Steller sea lions and northern fur seals: implications for the evolution of mammalian feeding. *Journal of Experimental Biology* **218**, 3229–3240.

Marshall, C. D., Wieskotten, S., Hanke, W., Hanke, F. D., Marsh, A., Kot, B. and Dehnhardt, G. (2014). Feeding kinematics, suction, and hydraulic jetting performance of harbor seals (*Phoca vitulina*). *PLoS ONE* **9**, e86710.

McGovern, K., Rodriguez, D. H., Lewis, M. N. and Davis, R. (2019). Diving classification and behavior of free-ranging female southern elephant seals based on three-dimensional movements and video-recorded observations. *Marine Ecology Progress Series* **620**, 215–232.

Naito, Y., Costa, D. P., Adachi, T., Robinson, P. W., Fowler, M. and Takahashi, A. (2013). Unravelling the mysteries of a mesopelagic diet: a large apex predator specializes on small prey. *Functional Ecology* **27**, 710-717.

Nordøy, E. S. and Blix, A. S. (2000). Distribution and food consumption of ross seals (*Ommatophoca rossi*) and leopard seals (*Hydrurga leptonyx*). *Norwegian Antarctic Research Expedition (NARE) 2000/2001* **Report 120**.

Pampush, J. D., Winchester, J. M., Morse, P. E., Vining, A. Q., Boyer, D. M. and Kay, R. F. (2016). Introducing molaR: a new R package for quantitative topographic analysis of teeth (and other topographic surfaces). *Journal of Mammalian Evolution* **23**, 397-412.

Pauly, D., Trites, A., Capuli, E. and Christensen, V. (1998). Diet composition and trophic levels of marine mammals. *ICES journal of Marine Science* **55**, 467-481.

Pyenson, N. D. (2017). The ecological rise of whales chronicled by the fossil record. *Current Biology* **27**, R558-R564.

Ross, G. J. B., Ryan, F., Saayman, G. S. and Skinner, J. (1976). Observations on two captive crabeater seals at the Port Elizabeth Oceanarium: *Lobodon carcinophagus*. *International Zoo Yearbook* **16**, 160-164.

Shapiro, S. S. and Wilk, M. B. (1965). An analysis of variance test for normality (complete samples). *Biometrika* **52**, 591-611.

Uhen, M. D. (2007). Evolution of marine mammals: back to the sea after 300 million years. *The Anatomical Record* **290**, 514–522.

Uhen, M. D. (2018). Dental morphology. In *Encyclopedia of Marine Mammals*, eds. B. Würsig J. G. M. Thewissen and K. M. Kovacs), pp. 246-250. London: Academic Press.

Ungar, P. S. (2010). Mammal teeth: origin, evolution, and diversity. Baltimore: Johns Hopkins University Press.

Ungar, P. S. and M'Kirera, F. (2003). A solution to the worn tooth conundrum in primate functional anatomy. *Proceedings of the National Academy of Sciences* **100**, 3874-3877.

van den Hoff, J. and Thalmann, S. (2020). Direct at-sea observations of elephant seals (*Mirounga* spp.) to help interpret digital bio-logging data. *The Open Biology Journal* **8**.

Weijs, W. (1994). Evolutionary approach of masticatory motor patterns in mammals. In *Biomechanics of feeding in vertebrates*, pp. 281-320: Springer.

Whitenack, L. B. and Motta, P. J. (2010). Performance of shark teeth during puncture and draw: implications for the mechanics of cutting. *Biological Journal of the Linnean Society* **100**, 271–286.

Wickham, H., Francois, R., Henry, L. and Müller, K. (2016). dplyr: A grammar of data manipulation: Available from: https://CRAN.R-project.org/package=dplyr.

Winchester, J. M., Boyer, D. M., St Clair, E. M., Gosselin-Ildari, A. D., Cooke, S. B. and Ledogar, J. A. (2014). Dental topography of platyrrhines and prosimians: convergence and contrasts. *Am J Phys Anthropol* **153**, 29-44.

Figures and Tables

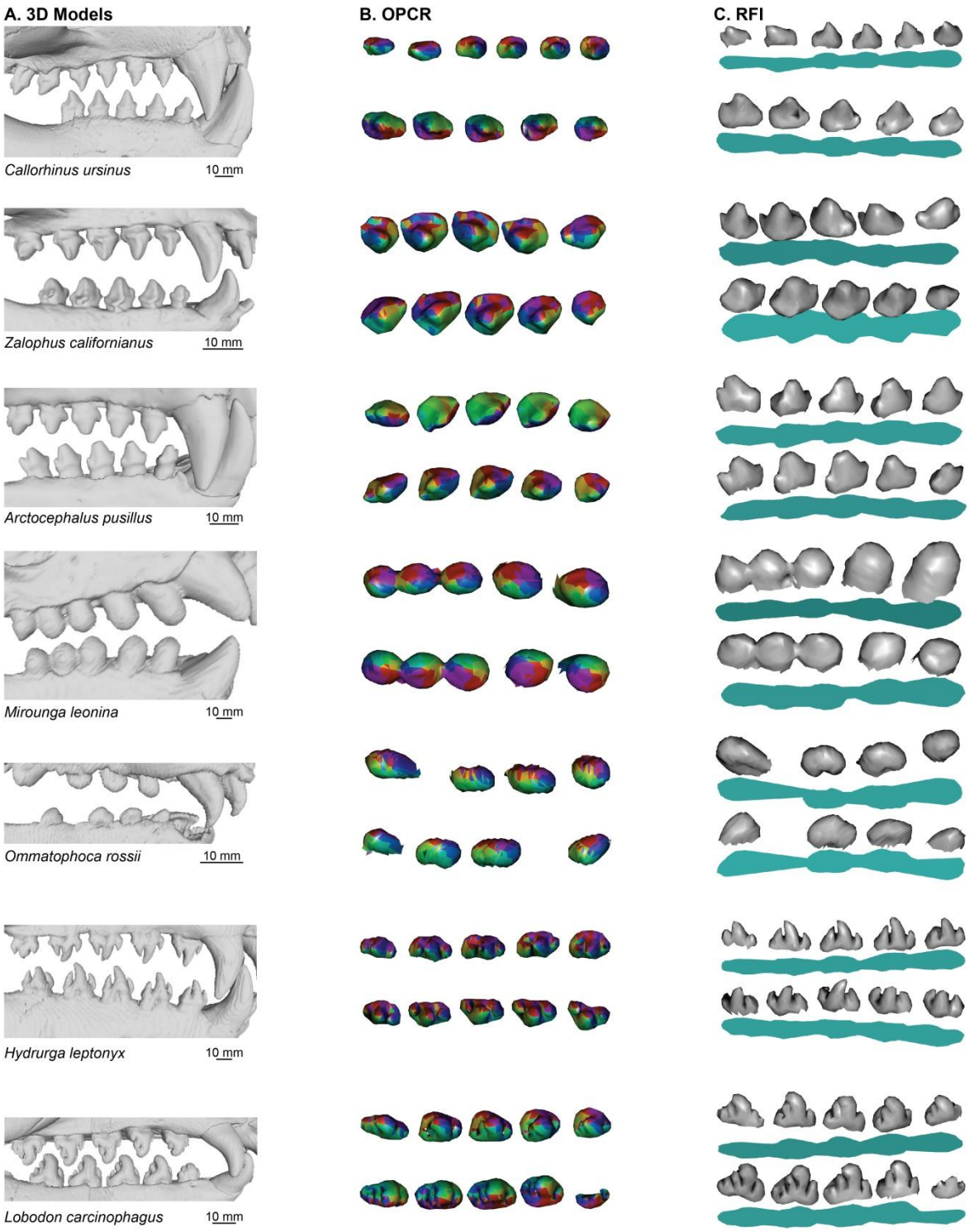

Figure 1: Digital reconstructions of each tooth row used in this analysis visualized as (A.) 3D Computed Tomography (CT) models, (B.) Orientation Patch Count (OPCR), and (C.) the Relief Index (RFI). Specimens in this analysis are: USNM 219817 *Callorhinus ursinus*; LACM 095730 *Zalophus californianus*; NMVC 5717 *Arctocephalus pusillus*; USNM 239141 *Mirounga leonina*; USNM 275206 *Ommatophoca rossii*; USNM 269533 *Hydrurga leptonyx*; and USNM 550078 *Lobodon carcinophagus*.

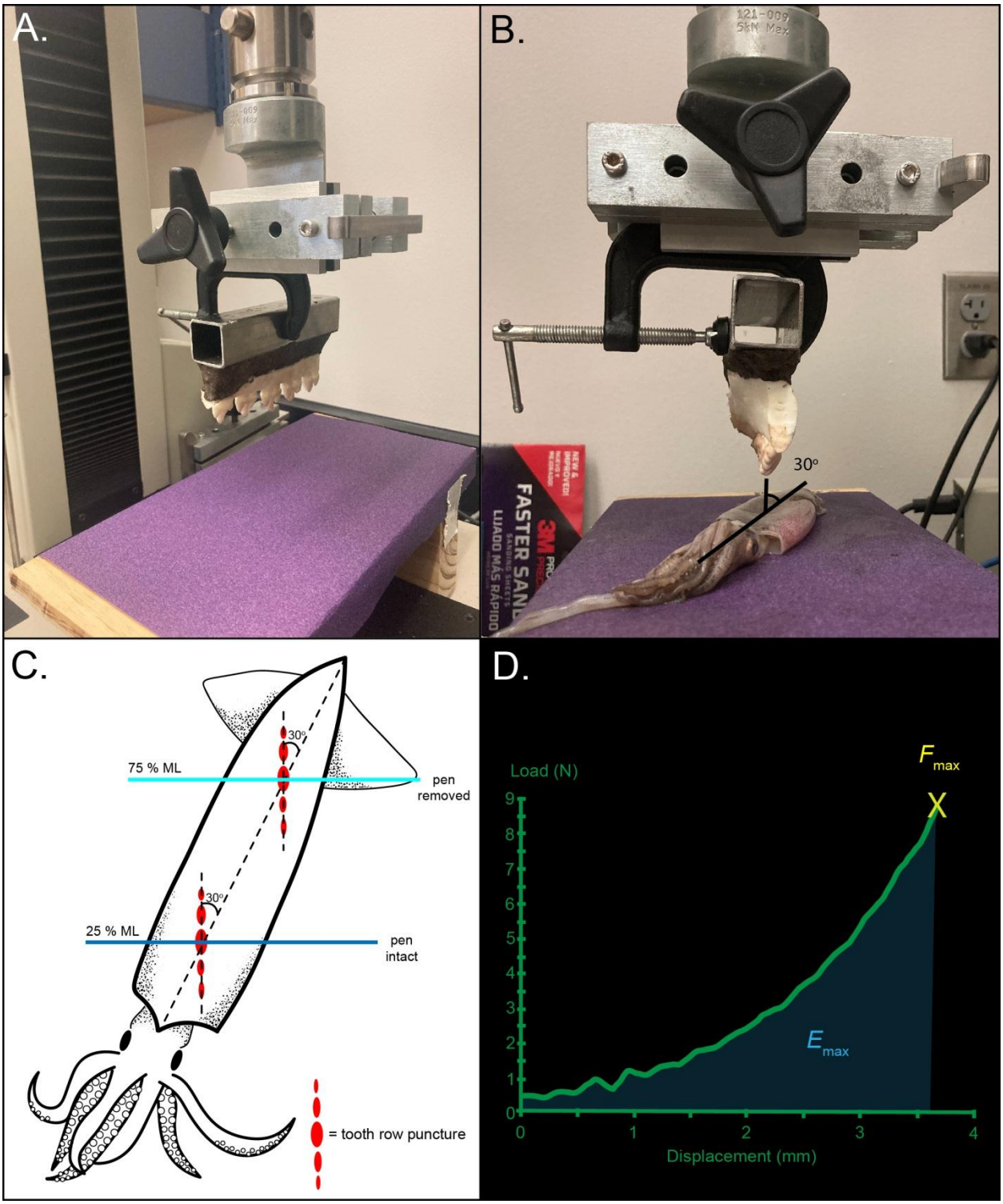

Figure 2: Experimental setup for punction performance testing in (A.) oblique and (B.) anterior views. (C.) schematic representation of a squid (*Loligo sp.*) demonstrating the position on the mantle at which the tooth models penetrated the squid. ML = mantle length. (D.) Representative load-displacement curve from a puncture test, from which maximum puncture force (F_{max}) and energy to maximum puncture force (E_{max}) were calculated. All puncture tests were terminated when the apex of the longest tooth from the tooth row reached a distance of 3 mm above the specimen support.

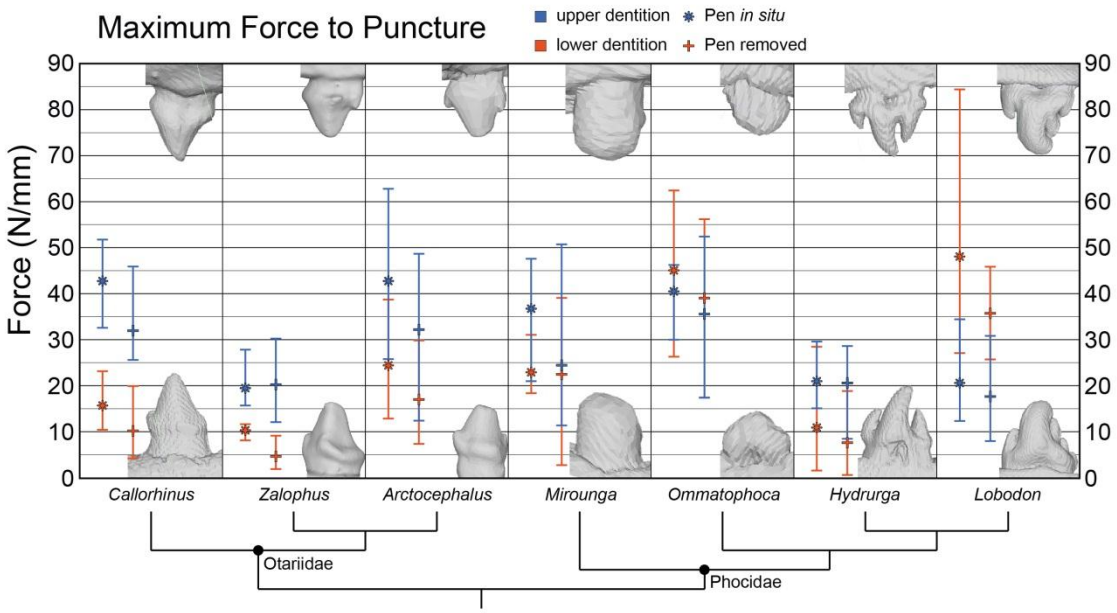

Figure 3: Results for the maximum force to puncture (F_{max}) in Newtons per millimeter for each of the seven taxa in this study. Values were log transformed for the statistical tests but original values are displayed in this figure. The blue color denotes a taxon's upper dentition while the orange color denotes the lower dentition. * = mean of all five trials with the pen *in situ*. + = mean of all five trials with the pen removed. Bars = range of all five trials.

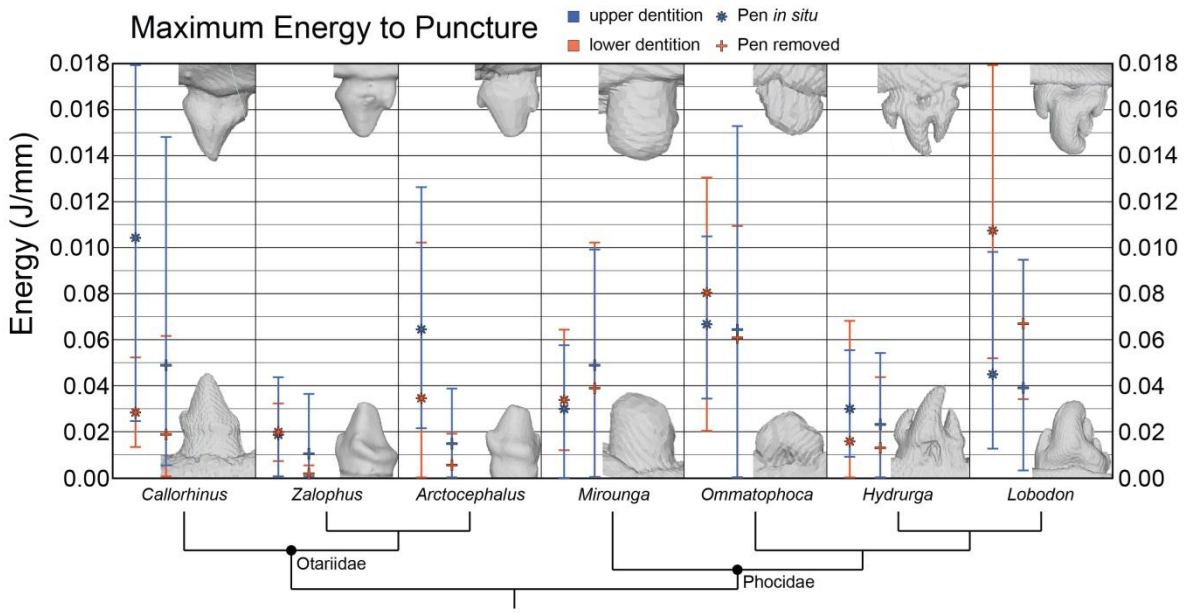

Figure 4: Results for the maximum force to puncture (E_{max}) in Joules per millimeter for each of the seven taxa in this study. Values were log transformed for the statistical tests but original values are displayed in this figure. The blue color denotes a taxon's upper dentition while the orange color denotes the lower dentition. * = mean of all five trials with the pen *in situ*. + = mean of all five trials with the pen removed. Bars = range of all five trials.

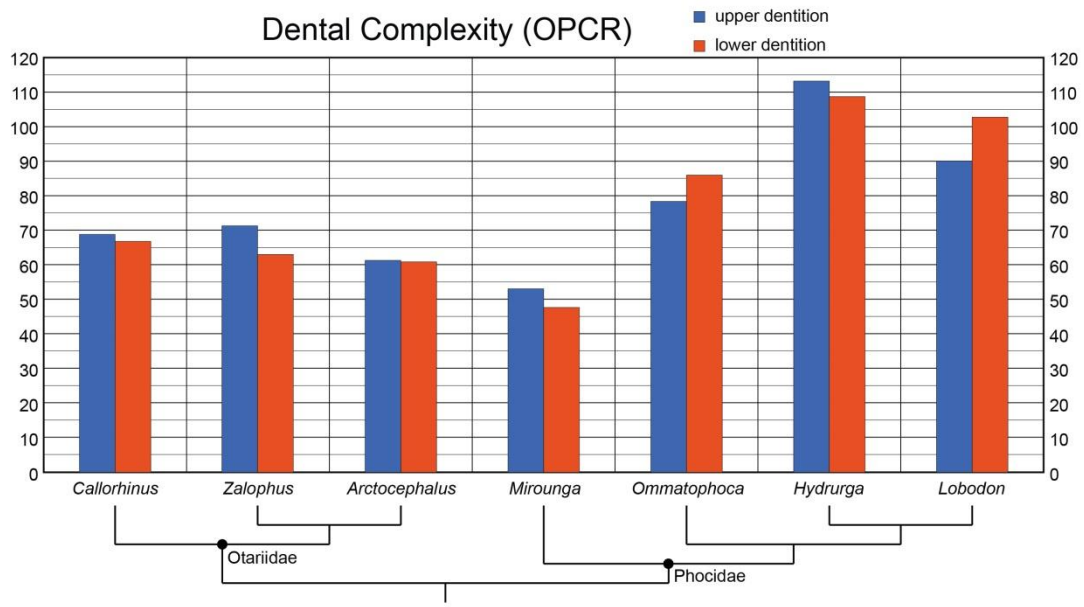

Figure 5: Pinniped dental complexity, measured by Orientation Patch Count Rotated (OPCR) following Pampush et al. (2016), for each of the seven taxa in this study. The blue color denotes a taxon's upper dentition while the orange color denotes the lower dentition. The individual orientation of each patch is depicted in Figure 1.

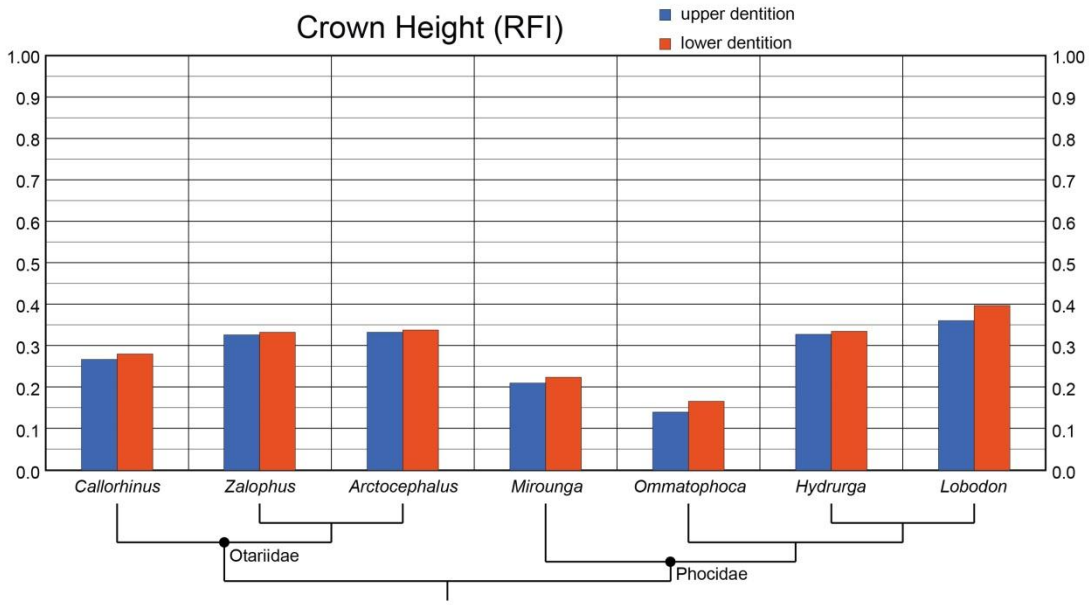

Figure 6: Pinniped crown height, measured by Relief Index (RFI) following Pampush et al. (2016), for each of the seven taxa in this study. The blue color denotes a taxon's upper dentition while the orange color denotes the lower dentition. The relationship between the 2D footprint and the 3D surface area is depicted in Figure 1.

Table 1: Maximum force to puncture (F_{max}) as measured in N/mm of five trials for each tooth row with the pen *in situ*. **U/L** = upper or lower tooth rows; **L/R** = left or right tooth rows; **T1–T5** = performance trials; $\bar{x}$ = mean; **SE** = standard error for the five trials, respectively.

Specimen	Taxon	U/L	L/R	T1	T2	T3	T4	T5	$\bar{x}$	SE
USNM 219817	*Callorhinus ursinus*	L	L	12.97	12.09	23.12	17.82	11.37	15.47	2.219
USNM 219817	*Callorhinus ursinus*	U	L	44.28	33.50	35.97	52.99	52.08	43.77	4.004
NMVC 5717	*Arctocephalus pusillus*	L	R	18.09	23.66	13.45	38.80	26.54	24.11	4.311
NMVC 5717	*Arctocephalus pusillus*	U	L	63.67	30.67	47.27	42.92	26.54	42.21	6.579
LACM 095730	*Zalophus californianus*	L	L	11.56	10.26	10.72	8.21	10.56	10.26	0.556
LACM 095730	*Zalophus californianus*	U	L	20.70	17.76	16.01	17.36	27.12	19.79	1.986
USNM 239141	*Mirounga leonina*	L	L	24.63	31.49	18.28	19.03	21.95	23.08	2.386
USNM 239141	*Mirounga leonina*	U	L	47.62	37.50	21.39	36.85	36.90	36.05	4.196
USNM 275206	*Ommatophoca rossii*	L	R	58.44	44.37	26.36	37.35	62.53	45.81	6.675
USNM 275206	*Ommatophoca rossii*	U	R	30.56	41.36	44.95	46.25	42.24	41.07	2.773
USNM 269533	*Hydrurga leptonyx*	L	L	4.77	7.23	2.23	28.52	9.91	10.53	4.674
USNM 269533	*Hydrurga leptonyx*	U	L	29.84	23.65	24.33	16.74	15.19	21.95	2.680
USNM 550078	*Lobodon carcinophagus*	L	L	84.56	27.89	40.99	33.33	55.00	48.35	10.134
USNM 550078	*Lobodon carcinophagus*	U	L	34.14	16.94	12.78	23.95	13.95	20.35	3.956

Table 2: Maximum force to puncture (F_{max}) as measured in N/mm of five trials for each tooth row with the pen removed. **U/L** = upper or lower tooth rows; **L/R** = left or right tooth rows; **T1–T5** = performance trials; $\bar{x}$ = mean; **SE** = standard error for the five trials, respectively.

Specimen	Taxon	U/L	L/R	T1	T2	T3	T4	T5	$\bar{x}$	SE
USNM 219817	*Callorhinus ursinus*	L	L	4.10	5.97	20.72	10.95	8.88	10.12	2.900
USNM 219817	*Callorhinus ursinus*	U	L	30.65	26.72	32.80	26.88	46.31	32.67	3.598
NMVC 5717	*Arctocephalus pusillus*	L	R	11.84	11.72	6.94	26.69	30.01	17.44	4.571
NMVC 5717	*Arctocephalus pusillus*	U	L	48.73	12.92	27.33	43.04	30.01	32.41	6.288
LACM 095730	*Zalophus californianus*	L	L	8.78	3.28	2.56	5.77	2.30	4.54	1.225
LACM 095730	*Zalophus californianus*	U	L	12.60	30.14	30.74	12.57	18.28	20.86	4.047
USNM 239141	*Mirounga leonina*	L	L	31.11	12.34	16.87	11.51	50.99	24.56	7.484
USNM 239141	*Mirounga leonina*	U	L	43.57	29.90	45.91	25.77	37.25	36.48	3.859
USNM 275206	*Ommatophoca rossii*	L	R	47.10	35.46	17.53	42.27	56.47	39.76	6.527
USNM 275206	*Ommatophoca rossii*	U	R	17.22	51.99	48.81	26.94	32.30	35.45	6.583
USNM 269533	*Hydrurga leptonyx*	L	L	0.86	4.52	3.39	19.65	8.64	7.41	3.307
USNM 269533	*Hydrurga leptonyx*	U	L	28.03	23.43	24.30	8.18	20.82	20.95	3.395
USNM 550078	*Lobodon carcinophagus*	L	L	43.57	29.90	45.91	25.77	37.25	36.48	3.859
USNM 550078	*Lobodon carcinophagus*	U	L	22.76	16.26	7.68	30.60	11.50	17.76	4.080

Table 3: Maximum energy to puncture (E_{max}) as measured in J/mm of five trials for each tooth row with the pen *in situ*. **U/L** = upper or lower tooth rows; **L/R** = left or right tooth rows; **T1–T5** = performance trials; $\bar{x}$ = mean; **SE** = standard error for the five trials, respectively.

Specimen	Taxon	U/L	L/R	T1	T2	T3	T4	T5	$\bar{x}$	SE
USNM 219817	*Callorhinus ursinus*	L	L	0.01	0.02	0.05	0.04	0.02	0.03	0.007
USNM 219817	*Callorhinus ursinus*	U	L	0.08	0.02	0.05	0.17	0.18	0.10	0.032
NMVC 5717	*Arctocephalus pusillus*	L	R	0.03	0.02	0.00	0.10	0.02	0.03	0.017
NMVC 5717	*Arctocephalus pusillus*	U	L	0.13	0.01	0.05	0.11	0.02	0.06	0.023
LACM 095730	*Zalophus californianus*	L	L	0.02	0.02	0.02	0.01	0.03	0.02	0.004
LACM 095730	*Zalophus californianus*	U	L	0.03	0.01	0.02	0.00	0.04	0.02	0.007
USNM 239141	*Mirounga leonina*	L	L	0.04	0.06	0.01	0.01	0.04	0.03	0.010
USNM 239141	*Mirounga leonina*	U	L	0.06	0.03	0.00	0.02	0.05	0.03	0.010
USNM 275206	*Ommatophoca rossii*	L	R	0.12	0.07	0.02	0.07	0.13	0.08	0.020
USNM 275206	*Ommatophoca rossii*	U	R	0.03	0.08	0.06	0.11	0.06	0.07	0.012
USNM 269533	*Hydrurga leptonyx*	L	L	0.00	0.00	0.00	0.07	0.02	0.02	0.013
USNM 269533	*Hydrurga leptonyx*	U	L	0.06	0.04	0.04	0.01	0.01	0.03	0.009
USNM 550078	*Lobodon carcinophagus*	L	L	0.17	0.05	0.07	0.07	0.18	0.11	0.027
USNM 550078	*Lobodon carcinophagus*	U	L	0.10	0.02	0.01	0.06	0.02	0.04	0.016

Table 4: Maximum energy to puncture (E_{max}) as measured in J/mm of five trials for each tooth row with the pen removed. **U/L** = upper or lower tooth rows; **L/R** = left or right tooth rows; **T1–T5** = performance trials; $\bar{x}$ = mean; **SE** = standard error for the five trials, respectively.

Specimen	Taxon	U/L	L/R	T1	T2	T3	T4	T5	$\bar{x}$	SE
USNM 219817	*Callorhinus ursinus*	L	L	0.00	0.00	0.06	0.02	0.02	0.02	0.009
USNM 219817	*Callorhinus ursinus*	U	L	0.03	0.01	0.03	0.05	0.15	0.05	0.021
NMVC 5717	*Arctocephalus pusillus*	L	R	0.00	0.00	0.00	0.02	0.01	0.01	0.003
NMVC 5717	*Arctocephalus pusillus*	U	L	0.04	0.00	0.00	0.03	0.01	0.02	0.006
LACM 095730	*Zalophus californianus*	L	L	0.01	0.00	0.00	0.00	0.00	0.00	0.001
LACM 095730	*Zalophus californianus*	U	L	0.00	0.04	0.01	0.00	0.00	0.01	0.006
USNM 239141	*Mirounga leonina*	L	L	0.02	0.08	0.00	0.00	0.10	0.04	0.018
USNM 239141	*Mirounga leonina*	U	L	0.00	0.00	0.00	0.00	0.10	0.02	0.016
USNM 275206	*Ommatophoca rossii*	L	R	0.07	0.04	0.00	0.09	0.10	0.06	0.015
USNM 275206	*Ommatophoca rossii*	U	R	0.00	0.14	0.15	0.01	0.02	0.06	0.027
USNM 269533	*Hydrurga leptonyx*	L	L	0.00	0.00	0.01	0.04	0.01	0.01	0.006
USNM 269533	*Hydrurga leptonyx*	U	L	0.05	0.03	0.03	0.00	0.01	0.02	0.006
USNM 550078	*Lobodon carcinophagus*	L	L	0.08	0.03	0.10	0.04	0.09	0.07	0.011
USNM 550078	*Lobodon carcinophagus*	U	L	0.06	0.03	0.00	0.10	0.01	0.04	0.014

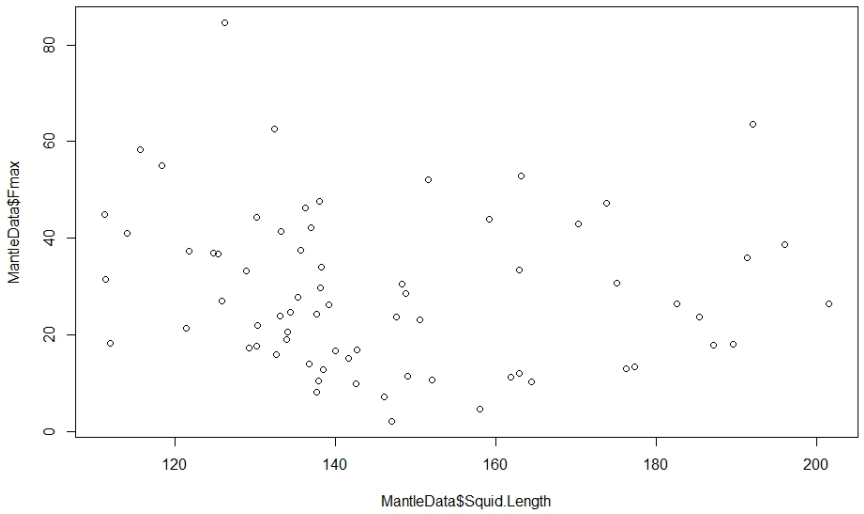

Fig. 1. Linear correlation between squid mantle length and maximum force to puncture (F_{max}). We found no correlation between squid mantle length and maximum force to puncture (Pearson's r = -0.117; t = -0.974; df = 68; p-value = 0.334).

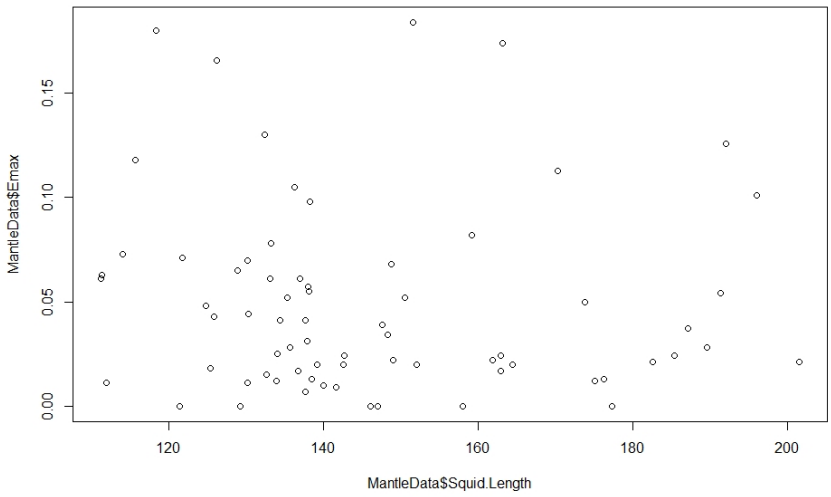

Fig. 2. Linear correlation between squid mantle length and maximum force to puncture (E_{max}). We found no correlation between squid mantle length and maximum energy to puncture (Pearson's r = -0.080; t = -0.663; df = 68; p-value = 0.510).

Table S1. Results for measures of dental complexity for the seven tooth rows used in this study. **OPCR** = Orientation Patch Count Rotated; **RFI** = Relief Index; **2DA** = the two-dimensional area of the tooth row's footprint; **3DA** = the three-dimensional surface area of the tooth crowns.

Specimen	Genus	Row	2DA	3DA	RFI	OPCR
USNM 219817	*Callorhinus ursinus*	Upper	291.6	491.2	0.26	68.75
USNM 219817	*Callorhinus ursinus*	Lower	235.3	416.4	0.29	66.25
NMVC 5717	*Arctocephalus pusillus*	Upper	399.3	808.6	0.35	61.62
NMVC 5717	*Arctocephalus pusillus*	Lower	354.0	764.8	0.39	61.12
LACM 095730	*Zalophus californianus*	Upper	7060.9	13838.1	0.34	70.25
LACM 095730	*Zalophus californianus*	Lower	6280.2	12703.6	0.35	63.25
USNM 239141	*Mirounga leonina*	Lower	298.6	467.3	0.22	53.12
USNM 239141	*Mirounga leonina*	Upper	302.4	497.7	0.25	47.00
USNM 275206	*Ommatophoca rossii*	Upper	225.8	301.2	0.14	77.62
USNM 275206	*Ommatophoca rossii*	Lower	202.6	280.2	0.16	85.50
USNM 269533	*Hydrurga leptonyx*	Upper	1130.4	2220.1	0.34	112.62
USNM 269533	*Hydrurga leptonyx*	Lower	1120.6	2557.5	0.37	109.62
USNM 550078	*Lobodon carcinophagus*	Upper	701.1	1466.1	0.39	90.00
USNM 550078	*Lobodon carcinophagus*	Lower	670.1	1471.5	0.39	103.00

Table S2. Results for Tukey's HST post-hoc tests of significance between individual tooth rows for the maximum force to puncture. Only significant comparisons are displayed, with groups indicating which tooth rows were significantly different from one another. Tukey's HSD results for all possible pairs are reported in Table S1.

Tooth Row	logFmax	groups
Ommatophoca Lowers	3.695	a
Lobodon Lowers	3.686	a
Callorhinus Uppers	3.613	ab
Ommatophoca Uppers	3.598	ab
Arctocephalus Uppers	3.539	ab
Mirounga Uppers	3.292	ab
Hydrurga Uppers	3.010	abc
Zalophus Uppers	2.964	abc
Mirounga Lowers	2.929	abc
Arctocephalus Lowers	2.915	abc
Lobodon Uppers	2.854	bc
Callorhinus Lowers	2.431	cd
Zalophus Lowers	1.849	d
Hydrurga Lowers	1.770	d

Table S3. Results for Tukey's HSD post-hoc tests of significance between individual tooth rows for the maximum force to puncture. **Diff** = difference in the mean values for the tooth rows; **lwr** = the lower 95% confidence interval; **upr** = the upper 95% confidence interval; **p adj** = p-value; **sig** = significance code: *** = 0; ** = 0.001; * = 0.01. Comparisons between tooth rows are ordered from most significant to least significant.

Click here to download Table S3

Table S4. Results for Tukey's HSD post-hoc tests of significance between individual tooth rows for the maximum energy to puncture. **Diff** = difference in the mean values for the tooth rows; **lwr** = difference in the minimum values for the tooth rows; **upr** = difference in the maximum values for the tooth rows; **p adj** = p-value; **sig** = significance code: *** = 0; ** = 0.001; * = 0.01. Comparisons between tooth rows are ordered from most significant to least significant.

Click here to download Table S4